

---

# TCE: A Test-Based Approach to Measuring Calibration Error

---

Takuo Matsubara<sup>1,2</sup>

Niek Tax<sup>3</sup>

Richard Mudd<sup>3</sup>

Ido Guy<sup>3</sup>

<sup>1</sup>The Alan Turing Institute

<sup>2</sup>Newcastle University

<sup>3</sup>Meta Platforms, Inc.

## Abstract

This paper proposes a new metric to measure the calibration error of probabilistic binary classifiers, called *test-based calibration error* (TCE). TCE incorporates a novel loss function based on a statistical test to examine the extent to which model predictions differ from probabilities estimated from data. It offers (i) a clear interpretation, (ii) a consistent scale that is unaffected by class imbalance, and (iii) an enhanced visual representation with respect to the standard reliability diagram. In addition, we introduce an optimality criterion for the binning procedure of calibration error metrics based on a minimal estimation error of the empirical probabilities. We provide a novel computational algorithm for optimal bins under bin-size constraints. We demonstrate properties of TCE through a range of experiments, including multiple real-world imbalanced datasets and ImageNet 1000.

## 1 INTRODUCTION

In recent years, it has become ubiquitous to deploy complex machine learning models in real-world production systems. Many of these systems rely on probabilistic classifiers that predict the probability that some target outcome occurs. For such systems, it is often crucial that their predictive probabilities are *well-calibrated*, meaning that the predictive probability accurately reflects the true frequency that the target outcome occurs. In some contexts, failures to achieve calibration can lead to negative consequences. In applications like medical diagnoses [Topol, 2019] and autonomous driving [Grigorescu et al., 2020], associated risks are often assessed based on model predictions and the consequences of a misguided risk evaluation can be severe. In online advertising auctions [Li et al., 2015], it is common to incorporate a prediction of the probability of some outcome of

interest (e.g., a click on an advert) when calculating an advertiser’s bid.

While a number of metrics—such as log-likelihood, user-specified scoring functions, and the area under the receiver operating characteristic (ROC) curve—are used to assess the quality of probabilistic classifiers, it is usually hard or even impossible to gauge whether predictions are well-calibrated from the values of these metrics. For assessment of calibration, it is typically necessary to use a metric that measures *calibration error*, that is, a deviation between model predictions and probabilities of target occurrences estimated from data. The importance of assessing calibration error has been long emphasised in machine learning [Nixon et al., 2019, Minderer et al., 2021] and in probabilistic forecasting more broadly [Dawid, 1982, Degroot and Fienberg, 1983].

However, existing metrics of calibration error have several drawbacks that in certain scenarios can mean that their values do not appropriately reflect true calibration performance. In particular, we will demonstrate that values of existing calibration error metrics have an inconsistent scale that is influenced by the target class proportion. In applications such as fraud detection [Abdallah et al., 2016, Tax et al., 2021] and advertising conversion prediction [Yang and Zhai, 2022], the prevalence, i.e., the proportion of instances belonging to the target class, is often very low. This leads to situations where one may be unable to identify whether the values of calibration error metrics are small due to good calibration performance or due to the low prevalence. This is also problematic for monitoring applications aimed at tracking the calibration performance of a model in a production system, where the prevalence can change over time (i.e., *prior probability shift* [Storkey et al., 2009]) and that makes it difficult to understand whether to attribute changes in the metric to an actual change in calibration performance or to the change in prevalence.

Furthermore, *binning* of model predictions—an essential component of most calibration error metrics [Naeini et al., 2015]—is often based on heuristics and lacks clear design

principles. For calibration error metrics, empirical probabilities of target occurrences are typically estimated by clustering data into several subsets based on binning of the associated model predictions. The design of the binning scheme is a vital factor in the accurate estimation of the empirical probabilities, yet few principles guiding the design of binning schemes have emerged to date.

In this paper, we elaborate on the issues of existing calibration error metrics in Section 2. We establish a simple yet novel metric that counterbalances the issues in Section 3. Section 4 empirically demonstrates properties of the proposed metric by experiments based on various datasets. Related works are discussed in Section 5, followed by the conclusion in Section 6. This paper focuses on the methodological aspects of the proposed new metric for binary classification, while theoretical development is left for future research. Our contributions are summarised as follows:

### Contributions

- Our primary contribution is a novel calibration error metric called *test-based calibration error* (TCE). TCE is based on statistical hypothesis testing and is interpretable as a percentage of model predictions that deviate significantly from estimated empirical probabilities. TCE produces values in a normalised, comparable range  $[0, 100]$  regardless of the class prevalence.
- We propose an explanatory visual representation of TCE called the *test-based reliability diagram*. It carries more information than the standard reliability diagram and facilitates a better understanding of calibration performance (See Figure 1).
- We introduce an optimality criterion for bins under which optimal bins minimise an estimation error of the empirical probabilities. We then propose a novel algorithm to compute optimal bins approximately under the constraints of the minimum and maximum size of each bin.

## 2 BACKGROUND

In this section, we introduce the definition of *calibration* and recap one of the most common *calibration error* metrics. We then outline several critical challenges of existing calibration error metrics. The basic notation used in this paper is introduced below.

Denote input and output spaces respectively by  $\mathcal{X}$  and  $\mathcal{Y}$ . We focus on probabilistic binary classification, i.e.  $\mathcal{Y} = \{0, 1\}$ , in which a probabilistic classifier  $P_\theta : \mathcal{X} \rightarrow [0, 1]$  models a conditional probability of  $Y = 1$  given an input  $x \in \mathcal{X}$ . The data  $\mathcal{D} := \{x_i, y_i\}_{i=1}^N$  are assumed to be i.i.d. realisations from a random variable  $(X, Y) \sim \mathbb{P}$ . To simplify notation, for any data subset  $S \subseteq \mathcal{D}$ , we denote by  $S^x$  a set of all inputs  $x$  in  $S$  and by  $S^y$  a set of all outputs  $y$  in  $S$ . By “a set of bins” or simply “bins”, we mean a set of arbitrary

disjoint intervals whose union is the unit interval  $[0, 1]$ . For example, a set  $\{\Delta_b\}_{b=1}^2$  of intervals  $\Delta_1 = [0.0, 0.4]$  and  $\Delta_2 = [0.4, 1.0]$  is a set of bins.

### 2.1 CALIBRATION ERROR

A probabilistic classifier  $P_\theta : \mathcal{X} \rightarrow [0, 1]$  is said to be *calibrated* [Dawid, 1982, Bröcker, 2009] if

$$\mathbb{P}(Y = 1 \mid P_\theta(X) = Q) = Q \quad (1)$$

for all  $Q \in [0, 1]$  s.t. the conditional probability is well-defined. Informally, this criterion implies that the model prediction coincides with the actual probability of  $Y = 1$  for all inputs. Any deviation between the actual probabilities and the model predictions in eq. (1) is often referred to as *calibration error*, which quantifies to what degree the classifier  $P_\theta$  is calibrated. The empirical computation of such a deviation involves estimating conditional probability  $\mathbb{P}(Y = 1 \mid P_\theta(X) = Q)$  from data. For given bins  $\{\Delta_b\}_{b=1}^B$ , define disjoint subsets  $\{\mathcal{D}_b\}_{b=1}^B$  of data  $\mathcal{D}$  by

$$\mathcal{D}_b := \{(x_i, y_i) \in \mathcal{D} \mid P_\theta(x_i) \in \Delta_b\}. \quad (2)$$

Simply put,  $\mathcal{D}_b$  is a subset of data whose model predictions have similar values. The conditional probability  $\mathbb{P}(Y = 1 \mid P_\theta(X) = Q)$  for any  $Q \in \Delta_b$  can then be estimated by the empirical mean of the labels in subset  $\mathcal{D}_b$ :

$$\mathbb{P}(Y = 1 \mid P_\theta(X) = Q) \approx \hat{P}_b := \frac{1}{N_b} \sum_{y_i \in \mathcal{D}_b^y} y_i \quad (3)$$

where we denote by  $\hat{P}_b$  the estimated conditional probability in  $\mathcal{D}_b$  and by  $N_b$  the sample size of  $\mathcal{D}_b$ .

One of the most common metrics to measure calibration error is *expected calibration error* (ECE) [Naeini et al., 2015]. ECE uses equispaced bins  $\{\Delta_b\}_{b=1}^B$  over  $[0, 1]$  for a given number  $B$  and measures an absolute difference between the averaged model predictions and the estimated conditional probability  $\hat{P}_b$  within each data subset  $\mathcal{D}_b$ . The value of ECE is defined as

$$\text{ECE} := \sum_{b=1}^B \frac{N_b}{N} \left| \hat{P}_b - \frac{1}{N_b} \sum_{x_i \in \mathcal{D}_b^x} P_\theta(x_i) \right|. \quad (4)$$

ECE has an associated practical visual representation known as the *reliability diagram* [Degroot and Fienberg, 1983, Niculescu-Mizil and Caruana, 2005], which aligns the averaged model prediction and the estimated conditional probability in each  $\mathcal{D}_b$  (see Figure 1). The reliability diagram is a powerful tool to intuitively grasp the deviation between the model and the estimated probability in ECE.

### 2.2 CHALLENGES IN CALIBRATION ERROR

Calibration error metrics, such as ECE, are widely used in real-world applications. There nonetheless exist several

challenges that may cause a misassessment of calibration. These problems become evident especially when a distribution of model predictions  $\{P_\theta(x_i)\}_{i=1}^N$  is not well-dispersed. This scenario often arises in imbalanced classification where model predictions tend to be severely skewed towards either 0 or 1. The following paragraphs illustrate challenges of existing calibration error metrics, which we aim to address.

**Challenge 1 (Scale-Dependent Interpretation)** In most calibration error metrics, the deviation between the model prediction and the estimated probability  $\hat{P}_b$  in each  $\mathcal{D}_b$  is measured by the absolute difference as in eq. (4). However, the use of the absolute difference can result in values that have an inconsistent scale influenced by the class prevalence. To illustrate this problem, consider an estimated probability  $\hat{P}_b$  and an averaged model prediction denoted  $\bar{Q}_b$  for some  $b$  in eq. (4). If  $\hat{P}_b = 0.50$  and  $\bar{Q}_b = 0.49$ , their absolute difference is 0.01. On the other hand, if  $\hat{P}_b = 0.01$  and  $\bar{Q}_b = 0.0001$ , their absolute difference is 0.0099. Despite the comparison under the absolute difference suggesting that the probability  $\bar{Q}_b = 0.0001$  with respect to  $\hat{P}_b = 0.01$  in the latter case is better calibrated than in the former case, one may reasonably argue that the latter is not well-calibrated—or at least not comparable to the former—given the stark difference in the order of magnitude. Similarly to this illustration, the values of existing calibration metrics built on the absolute difference can be proportionally small whenever the scales of  $\hat{P}_b$  and  $\bar{Q}_b$  are small. This issue makes it difficult to distinguish whether the metric values are low due to good calibration performance or due to the small scale of the probabilities as in imbalanced classification.

**Challenge 2 (Lack of Normalised Range)** The range of values of calibration error metrics built on absolute differences is not normalised. The range can vary depending on the choice of bins  $\{\Delta_b\}_{b=1}^B$ . To illustrate this problem, consider a bin  $\Delta_b$  for some  $b$ . If  $\Delta_b = [0.4, 0.6]$ , the absolute difference between  $\hat{P}_b$  and  $\bar{Q}_b$  falls into a range  $[0.0, 0.6]$  because  $\hat{P}_b$  is the estimated probability in  $[0.0, 1.0]$  and the averaged model prediction  $\bar{Q}_b$  in the bin  $\Delta_b$  takes the value within  $\Delta_b$ . Similarly, a different choice of bin  $\Delta_b$  leads to a different range of the absolute difference. Consequently, the choice of bins  $\{\Delta_b\}_{b=1}^B$  impacts the range of the final value of calibration error metrics that are built on the absolute difference. To assure rigorous comparability of the final value of a calibration error metric, it is desirable to establish a measurement of the deviation whose value has a fixed, normalised range independent of the choice of bins.

**Challenge 3 (Arbitrary Choice of Bins)** An appropriate choice of bins is critical because it meaningfully impacts on final values of calibration error metrics. Equispaced bins  $\{\Delta_b\}_{b=1}^B$  over  $[0, 1]$  for a given number  $B$  are one of the most common choices of bins in practice, as used in ECE. However, equispaced bins can often cause a situation where

a few particular bins contain the majority of the model predictions when they are not well-dispersed over  $[0, 1]$ , as often happens in imbalanced classification. If some bin  $\Delta_b$  contains the majority of model predictions, the corresponding estimated probability  $\hat{P}_b$  coincides approximately with the empirical mean of all labels. On the other hand, estimated probabilities of the bins other than  $\Delta_b$  become unreliable due to the small size of samples contained. A potential solution to this problem is to use bins that adapt based on the dispersion of model predictions. Nixon et al. [2019] proposed *adaptive calibration error* (ACE) that computes the value of eq. (4) using bins  $\{\Delta_b\}_{b=1}^B$  based on  $B$ -quantiles of model predictions  $\{P_\theta(x_i)\}_{i=1}^N$  for given  $B$ . However, questions remain regarding the optimal number  $B$  of bins and the appropriate quantile to use for each bin. To the best of our knowledge, there is no established notion of what makes bins optimal, nor do clear design principles for bins exist.

### 3 CALIBRATION ERROR BASED ON TEST AND OPTIMAL BINS

We propose a new calibration error metric that offers a simple yet novel solution to the challenges outlined in Section 2.2. First, in Section 3.1, we present a general formulation of calibration error metrics that encompasses most metrics used in practice. This general formulation allows for a structured understanding of the design of calibration error metrics. In Section 3.2, we derive from the general formulation a new calibration error metric, called TCE, which incorporates a loss based on a statistical test to compare model predictions with estimated empirical probabilities. TCE produces a value that has a clear interpretation as a percentage of model predictions determined to deviate significantly from estimated empirical probabilities, which leads to a normalised range of possible values  $[0, 100]$  regardless of the choice of bins  $\{\Delta_b\}_{b=1}^B$ . In Section 3.3, we consider an optimal criterion of bins  $\{\Delta_b\}_{b=1}^B$  from the perspective of minimising an estimation error of the empirical probabilities  $\{\hat{P}_b\}_{b=1}^B$ . We then develop a practical regularisation approach that ensures a minimum and maximum sample size in each subset  $\mathcal{D}_b$ .

#### 3.1 GENERAL CALIBRATION ERROR

The following definition presents an abstract formulation of calibration error metrics, which we call *general calibration error* (GCE) for terminological convenience. Denote by  $2^{\mathcal{D}}$  a power set of  $\mathcal{D}$ , i.e. a space of all subsets of  $\mathcal{D}$  and by  $\mathcal{M}$  a space of all probabilistic classifiers below.

**Definition 1. (GCE)** Let  $L : 2^{\mathcal{D}} \times \mathcal{M} \rightarrow \mathbb{R}$  be a loss of any probabilistic classifier evaluated for any data subset. Let  $\mathcal{B}$  be a set of bins  $\{\Delta_b\}_{b=1}^B$  that define data subsets  $\{\mathcal{D}_b\}_{b=1}^B$  as in eq. (2). Let  $\|\cdot\|$  be a norm of a  $B$ -dimensional vector

space. For a given probabilistic classifier  $P_\theta : \mathcal{X} \rightarrow [0, 1]$ , define a scalar  $GCE_b \in \mathbb{R}$  for each  $b = 1, \dots, B$  by

$$GCE_b := L(\mathcal{D}_b, P_\theta). \quad (5)$$

Then, GCE of the probabilistic classifier  $P_\theta$  is defined by

$$GCE = \|(GCE_1, \dots, GCE_B)\|. \quad (6)$$

This formulation translates the problem of designing a calibration error metric into a problem of choosing the tuple  $(L, \mathcal{B}, \|\cdot\|)$ . Most existing calibration error metrics used in practice can be derived by selecting an appropriate tuple of the loss  $L$ , the bins  $\mathcal{B}$ , and the norm  $\|\cdot\|$  in GCE. See Example 1 below for the case of ECE. It is also immediate to show that ACE can be recovered from GCE.

**Example 1.** Let  $\mathcal{B}$  be equispaced bins  $\{\Delta_b\}_{b=1}^B$  over  $[0, 1]$ , let  $L$  be  $L(\mathcal{D}_b, P_\theta) = |\frac{1}{N_b} \sum_{y \in \mathcal{D}_b^y} y - \frac{1}{N_b} \sum_{x \in \mathcal{D}_b^x} P_\theta(x)|$ , and let  $\|\cdot\|$  be a weighted 1-norm  $\|v\| = \sum_{b=1}^B \frac{N_b}{N} \times |v_b|$ . The ECE corresponds to the GCE under this tuple.

We aim to choose the tuple  $(L, \mathcal{B}, \|\cdot\|)$  so that it addresses the aforementioned challenges in Section 2.2. Section 3.2 addresses a loss  $L$  based on a statistical test and presents the resulting TCE. Subsequently, Section 3.3 addresses a choice of bins  $\mathcal{B}$  that is obtained through optimisation to minimise an estimation error of the empirical probabilities  $\{\hat{P}_b\}_{b=1}^B$ . All norms  $\|\cdot\|$  are equivalent in finite dimensions, and hence we do not focus on any particular choice. As with ECE, we use the weighted 1-norm  $\|\cdot\|$  in Example 1 for TCE.

### 3.2 TEST-BASED CALIBRATION ERRORS

We present our main contribution, a new calibration error metric called TCE, that is derived from GCE by specifying a novel loss  $L$  based on a statistical test. Our proposed loss  $L$  summarises the percentage of model predictions that deviate significantly from the empirical probabilities in each subset  $\mathcal{D}_b$ . We effectively test a null hypothesis “the probability of  $Y = 1$  is equal to  $P_\theta(x)$ ” at each  $x \in \mathcal{D}_b^x$  using the output data  $\mathcal{D}_b^y$ . A rigorous formulation of this loss  $L$  is provided below, combined with the definition of the TCE. Note that the bins  $\{\Delta_b\}_{b=1}^B$  and the norm  $\|\cdot\|$  of TCE are arbitrary, while the weighted 1-norm is our default choice of  $\|\cdot\|$ .

**Definition 2. (TCE)** Given a statistical test and its significance level  $\alpha \in [0, 1]$ , let  $R$  be a function of any observed dataset of random variable  $Y \in \{0, 1\}$  and any probability  $Q \in [0, 1]$ , which returns 1 if a hypothesis  $P(Y = 1) = Q$  is rejected based on the dataset and returns 0 otherwise. In Definition 1, let  $L$  be an average rejection percentage s.t.

$$L(\mathcal{D}_b, P_\theta) = 100 \times \frac{1}{N_b} \sum_{x \in \mathcal{D}_b^x} R(\mathcal{D}_b^y, P_\theta(x)). \quad (7)$$

GCE in Definition 1 is then called TCE.

In contrast to existing metrics that examine the difference between averaged model predictions and empirical probabilities in each bin, TCE examines each prediction  $P_\theta(x)$  and summarises the rejection percentage in each bin. The procedure of TCE can be intuitively interpreted as follows.

**Remark 1.** Informally speaking, TCE examines whether each model prediction  $P_\theta(x)$  can be regarded as an outlier relative to the empirical probability of the corresponding data  $\mathcal{D}_b^y$ , where the test in function  $R$  acts as a criterion for determining outliers. The level of model-calibration is then measured by the rate of outliers produced by the model.

In this paper, we use the Binomial test as the *de facto* standard statistical test to define  $R$  in the TCE. TCE based on other tests, including Bayesian testing approaches, is an open direction for future research. Algorithm 1 summarises the computational procedure of TCE. There are multiple advantages of TCE as follows.

**Advantage 1 (Clear Interpretation)** The final value of TCE has a clear interpretation as a percentage of model predictions that are determined by the test of choice (here the Binomial test) to deviate significantly from estimated empirical probabilities. Because the value is a percentage, the range of the value is normalised to  $[0, 100]$ .

**Advantage 2 (Consistent Scale)** The test evaluates the statistical deviation of data from a model prediction  $P_\theta(x)$  adaptively and appropriately for each scale of  $P_\theta(x)$  and data size  $N_b$ . Informally, TCE is the number of relative outliers determined for each  $P_\theta(x)$  adaptively. This endows the value with a consistent scale robust to class imbalance.

**Advantage 3 (Enhanced Visualisation)** TCE leads to a new visual representation that shows the distribution of model predictions, and the proportion of model predictions that deviate significantly from an empirical probability in each bin. See Figure 1 for the description and comparison with the standard reliability diagram.

---

#### Algorithm 1 Computation of TCE

---

**Input:** data  $\mathcal{D}$ , model  $P_\theta$ , norm  $\|\cdot\|$ , bins  $\{\Delta_b\}_{b=1}^B$ , function  $R$  based on a chosen test and significant level

**Output:** a value TCE  $\in \mathbb{R}$

**for**  $b = 1, \dots, B$  **do**

$\mathcal{D}_b \leftarrow \{(x_i, y_i) \in \mathcal{D} \mid P_\theta(x_i) \in \Delta_b\}$   $\triangleright$  make subset  
TCE<sub>*b*</sub>  $\leftarrow 0$

**for**  $x_i \in \mathcal{D}_b^x$  **do**

TCE<sub>*b*</sub>  $\leftarrow$  TCE<sub>*b*</sub> +  $R(\mathcal{D}_b^y, P_\theta(x_i))$   $\triangleright$  test each

**end for**

TCE<sub>*b*</sub>  $\leftarrow 100/N_b \times$  TCE<sub>*b*</sub>

**end for**

TCE  $\leftarrow \|(TCE_1, \dots, TCE_B)\|$

---

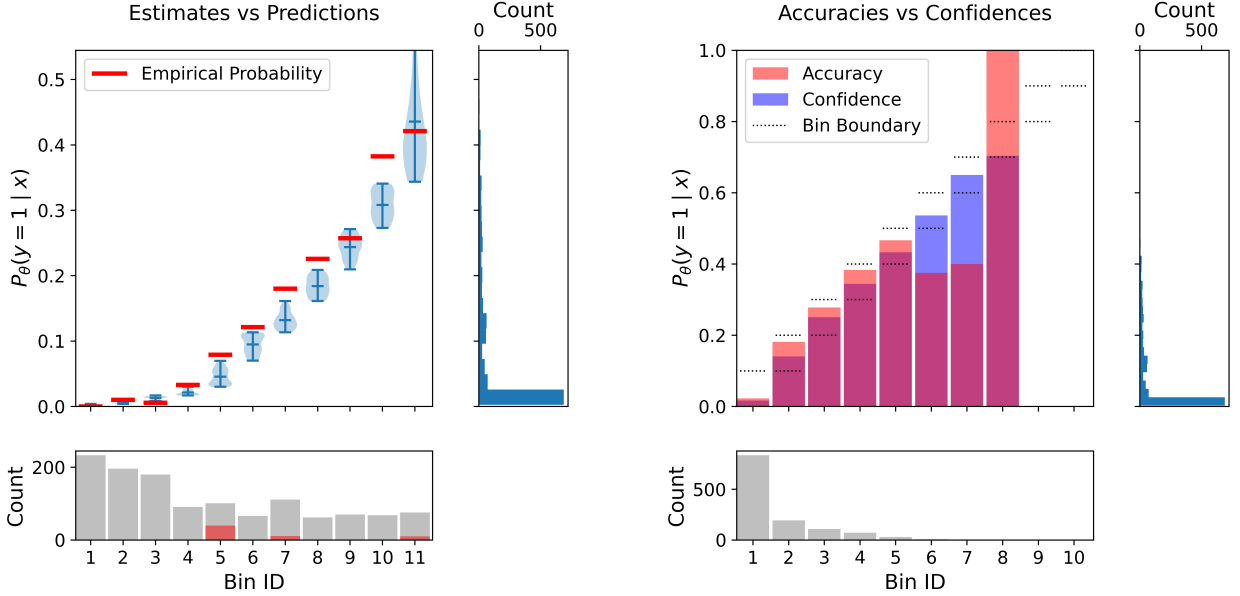


Figure 1: Comparison of two visual representations both applied for a gradient boosting model trained on the *abalone* dataset used in Section 4.2. (Left) A new visual representation, which we call the *test-based reliability diagram*. The central plot shows a violin plot of model predictions in each bin, whose estimated probability is presented by a red line. The bottom plot shows by grey bar the sample size of each bin and by red bar the percentage of model predictions that deviate significantly from the estimated probability in each bin. The right plot shows a histogram of all model predictions. (Right) The standard reliability diagram with the bin-size plot on the bottom and the histogram plot on the right added for comparison.

Our interest is in the aggregated rejection percentage of all the tests performed, and so multiple testing corrections—e.g., the Bonferroni correction to offer a frequentist guarantee to control the familywise error rate—are not considered. If all the null hypotheses were simultaneously true, TCE would simply coincide with the false positive rate which equals in expectation to type I error specified by the significant level of the test. Full discussion on when and how adjustments for multiple hypotheses tests should be made may be found in Bender and Lange [2001].

Given that TCE is based on a statistical testing procedure, it may be possible to apply ideas from power analysis to inform the desired sample size in each  $\mathcal{D}_b$ . Such analysis may also benefit the algorithm in the next subsection to compute optimal bins under the bin-size constraints, providing insights on what bin-size should be used as the constraints. Finally, it is worth noting that TCE can be extended to multi-class classification. The following remark presents one straightforward approach to the extension.

**Remark 2.** Any calibration error metric defined for binary classification can be extended to multi-class classification by considering classwise-calibration [e.g. Kull et al., 2019], where the calibration error metric is applied for one-vs-rest classification of each class independently. A modification of TCE in multi-class classification settings can then be defined as an average of TCEs applied for one-vs-rest classification of each class.

### 3.3 OPTIMAL BINS BY MONOTONIC REGRESSOR AND BIN-SIZE CONSTRAINTS

It is a fundamental challenge to establish a practical and theoretically sound mechanism to design bins used in calibration error metrics. Ideally designed bins provides accurate probability estimates  $\{\hat{P}_b\}_{b=1}^B$  from data  $\mathcal{D}$  while keeping the size of each bin reasonable. To this end, we propose a novel algorithm to compute bins that aim to minimise an estimation error of the probability estimates  $\{\hat{P}_b\}_{b=1}^B$  under the constraint of the size of each bin.

Recently, Dimitriadis et al. [2021] pointed out that an existing quadratic programming algorithm, called pool-adjacent-violators algorithm (PAVA), can be directly applied to compute “optimal” bins in the context of obtaining a better reliability diagram. The bins are designed in a manner that minimises the *Brier score* [Brier, 1950] of resulting empirical probabilities by virtue of PAVA. Forging ahead with this observation, we introduce the following definition that makes explicit in what sense bins  $\{\Delta_b\}_{b=1}^B$  can be considered optimal given an arbitrary estimation error  $D$  of the probability estimates  $\{\hat{P}_b\}_{b=1}^B$  from data  $\mathcal{D}$ .

**Definition 3. (Optimal Bins)** Let  $\Pi$  be a space of all sets of bins  $\{\Delta_b\}_{b=1}^B$  for any  $B$ , with associated data subsets denoted by  $\{\mathcal{D}_b\}_{b=1}^B$  and probability estimates from  $\{\mathcal{D}_b^y\}_{b=1}^B$  denoted by  $\{\hat{P}_b\}_{b=1}^B$ . Let  $D$  be any error function between an observed dataset of random variable  $Y \in \{0, 1\}$  and a

given probability  $Q \in [0, 1]$ . Any set of bins that satisfies

$$\min_{\{\Delta_b\}_{b=1}^B \in \Pi} \sum_{b=1}^B W_b \times D(\mathcal{D}_b^y, \hat{P}_b) \quad \text{subject to } \hat{P}_1 \leq \dots \leq \hat{P}_B \quad (8)$$

can be considered an optimal set of bins under the estimation error  $D$ , where  $W_b := N_b/N$  is the weight associated with the error of subset  $\mathcal{D}_b^y$  of size  $N_b$ .

The monotonic constraint  $\hat{P}_1 \leq \dots \leq \hat{P}_B$  of the probability estimates  $\{\hat{P}_b\}_{b=1}^B$  is a natural requirement because the choice of bins becomes trivial otherwise. For example, consider bins  $\{\Delta_b\}_{b=1}^B$  with  $B = N$  such that  $\Delta_b$  contains one single point  $y_b$  and the probability estimate  $\hat{P}_b = y_b$  for each  $b$ . This clearly achieves that  $\sum_{b=1}^B W_b \times D(\mathcal{D}_b^y, \hat{P}_b) = \frac{1}{N} \sum_{b=1}^N D(\{y_b\}, y_b) = 0$ . Under the monotonic constraint, the choice of bins becomes non-trivial.

Under some choices of the estimation error  $D$ , the optimisation of eq. (8) can be solved as a monotonic regression problem. Given an ordered dataset  $\{y_i\}_{i=1}^N$ , a monotonic regression algorithm finds  $N$  monotonically increasing values  $\hat{y}_1 \leq \dots \leq \hat{y}_N$  that minimise some loss between  $\{\hat{y}_i\}_{i=1}^N$  and  $\{y_i\}_{i=1}^N$ . There exist algorithms for various losses, including the  $l_p$  loss, the Huber loss, and the Chebyshev loss [de Leeuw et al., 2009]. PAVA solves a monotonic regression problem under the squared error  $\sum_{i=1}^N (\hat{y}_i - y_i)^2$ . If we choose the error  $D$  as the variance of each  $\mathcal{D}_b^y$ , i.e.,

$$D(\mathcal{D}_b^y, \hat{P}_b) = \frac{1}{N_b} \sum_{i=1}^{N_b} (y_i - \hat{P}_b)^2 \quad (9)$$

the optimal set of bins under  $D$  can be obtained using PAVA, which corresponds to the case of Dimitriadis et al. [2021]. See Appendix A for the proof that the optimisation criterion of eq. (8) is indeed minimised at bins obtained using PAVA. The approach using PAVA is a highly appealing solution to the design of bins  $\{\Delta_b\}_{b=1}^B$  because it achieves a fully-automated design of the bins based on the clear criterion of eq. (8). However, such a fully-automated design can occasionally generate a bin that contains an excessively small or large number of data for the sake of minimising the aggregated estimation error over all  $\{\hat{P}_b\}_{b=1}^B$ . Imposing a certain regularisation on the minimum and maximum size of each  $\mathcal{D}_b$  can aid in keeping some baseline quality of the estimation of each individual  $\hat{P}_b$ .

Therefore, we propose a modified version of PAVA that regularises based on the given minimum and maximum size of each subset  $\mathcal{D}_b^y$ . Algorithm 2 summarises the full algorithm, which we call *PAVA with block constraints* (PAVA-BC), followed by Algorithm 3 that summarises how to compute bins using PAVA-BC accordingly, where  $\text{Sort}(\mathcal{D}, P_\theta)$  in Algorithm 3 denotes any algorithm that sorts labels  $\{y_i\}_{i=1}^N$  in ascending order of model predictions  $\{P_\theta(x_i)\}_{i=1}^N$ . By

---

### Algorithm 2 PAVA-BC (PAVA with Block Constraints)

---

**Input:** ordered scalars  $\{y_i\}_{i=1}^N$ , size constraints  $N_{\min}$  and  $N_{\max}$  s.t.  $0 \leq N_{\min} \leq N_{\max} \leq N$ .

**Output:** sequence  $\{\hat{y}_i\}_{i=1}^N$

```

B ← 0
for i = 1, ..., N - Nmin do
  B ← B + 1
  YB ← yi
  WB ← 1
  while B > 1 do
    if WB-1 + WB > Nmin then
      if WB-1 + WB > Nmax then Break
      if YB-1/WB-1 < YB/WB then Break
    end if
    YB-1 ← YB-1 + YB
    WB-1 ← WB-1 + WB
    B ← B - 1
  end while
end for
if WB + Nmin ≤ Nmax then
  YB ← YB + ∑i=N-Nmin+1N yi
  WB ← WB + Nmin
else
  B ← B + 1
  YB ← ∑i=N-Nmin+1N yi
  WB ← Nmin
end if
s ← 0
for j = 1, ..., B do
  for k = 1, ..., Wj do
    ŷs+k ← Yj/Wj
  end for
  s ← s + Wj
end for

```

---



---

### Algorithm 3 Near-Optimal Bins Based on PAVA-BC

---

**Input:** data  $\mathcal{D}$ , model  $P_\theta$ , size constraints  $N_{\min}$  and  $N_{\max}$  s.t.  $0 \leq N_{\min} \leq N_{\max} \leq N$ .

**Output:** a set of bins  $\{\Delta_b\}_{b=1}^B$

```

{yi}i=1N ← Sort(ℳ, Pθ)
{ŷi}i=1N ← PAVA-BC({yi}i=1N, Nmin, Nmax)
B ← 1
L ← 0
R ← 0
for i = 2, ..., N do
  if ŷi-1 ≠ ŷi then
    R ← (Pθ(xi-1) + Pθ(xi))/2
    ΔB ← [L, R)
    L ← R
    B ← B + 1
  end if
end for
ΔB ← [L, 1.0]

```

---

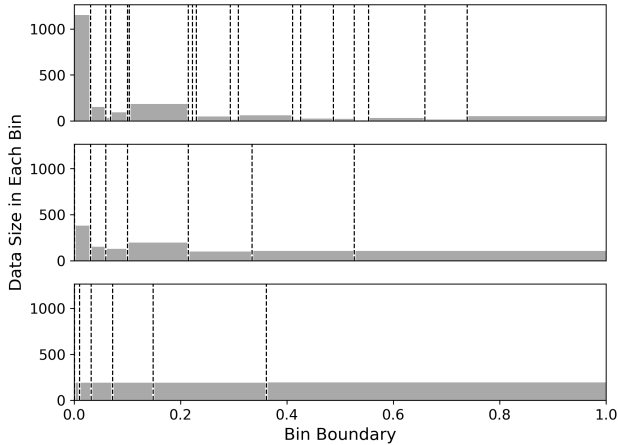


Figure 2: Comparison of bins for a random forest model on the *satimage* dataset used in Section 4.2 based on (top) PAVA, (middle) PAVA-BC, (bottom) binning based on 10-quantiles. The dotted line represents the boundary of each bin and the grey bar represents the size of each bin.

Algorithm 3, we can obtain bins that satisfy the given minimum and maximum size constraints  $N_{\min}$  and  $N_{\max}$  in each  $\mathcal{D}_b$ , while benefitting from the automated design of bins by PAVA. A set of bins based on PAVA can be recovered by replacing PAVA-BC with PAVA in Algorithm 3. In general, the introduction of the regularisation can cause mild violation of the monotonicity  $\hat{P}_1 \leq \dots \leq \hat{P}_B$ , meaning that there may exist a few values  $\hat{P}_b$  that is smaller than  $\hat{P}_{b-1}$ . See Appendix B for each example where mild violation of the monotonicity by PAVA-BC occurred and did not occur. In practice, mild violation of the monotonicity can often be a reasonable cost to achieve better properties of bins. For example, Tibshirani et al. [2011] studied settings where the monotonicity is only “nearly” satisfied.

See Figure 2 for a comparison of the bins computed by three different approaches: PAVA, PAVA-BC, and binning based on 10-quantiles. The bins produced by PAVA-BC interpolate between the optimal bins produced by PAVA and the well-sized bins produced by binning based on quantiles. This is further confirmed by Table 1 which shows the total estimation error in eq. (8) and the estimation error within each bin in eq. (9) for each approach. The total estimation error is minimised by PAVA, while an average of the estimation error within each bin is minimised by binning based on quantiles. In contrast, PAVA-BC takes a balance between the total and individual estimation error.

Table 1: The total estimation error and an average of the estimation error within each bin for the bins in Figure 2.

	PAVA	PAVA-BC	Quantile
Total Error	0.040	0.042	0.048
Averaged Within-Bin Error	0.132	0.077	0.047

## 4 EMPIRICAL EVALUATION

In this section, we demonstrate the properties of TCE via three experiments. The first experiment uses synthetic data to examine the properties of TCE under controlled class imbalance. The second experiment involves ten real-world datasets from the University of California Irvine (UCI) machine learning repository [Dua and Graff, 2017], where nine are designed as benchmark tasks of imbalanced classification, and one is a well-balanced classification task for comparison. In the second experiment, we also demonstrate that ECE and ACE may produce misleading assessments of calibration performance under class imbalance. TCE has the potential to reduce such misinterpretation risks. The final experiment uses the ImageNet1000 dataset to illustrate that TCE is applicable to large-scale settings. In all experiments, models are fitted to training data first and any calibration error metric are computed using validation data. Source code to reproduce the experiments is available in <https://github.com/facebookresearch/tce>.

We compute TCE with bins based on PAVA-BC unless otherwise stated. The minimum and maximum size of each bin for PAVA-BC are set to  $N/20$  and  $N/5$  for a given dataset size  $N$ . Under these constraints, the number of bins based on PAVA-BC falls into a range between 5 and 20. In addition to ECE and ACE, we include the maximum calibration error (MCE) [Naeini et al., 2015] for comparison. MCE is defined by replacing the weighted 1-norm with the supremum norm over  $b = 1, \dots, B$  in Example 1. We denote, by TCE(Q) and MCE(Q), TCE and MCE each with bins based on  $B$ -quantiles. For all metrics,  $B$ -equispaced bins and  $B$ -quantiles bins are computed with  $B = 10$ .

### 4.1 SYNTHETIC DATA WITH CONTROLLED CLASS IMBALANCE

We first examine TCE using synthetic data from a simulation model considered in Vaicenavicius et al. [2019]. The data are simulated from a Gaussian discriminant analysis model  $(x, y) \sim P(x | y)P(y)$ . The output  $y \in \{0, 1\}$  is first sampled from a Bernoulli distribution  $P(y)$  with parameter  $\pi$  and the input  $x \in \mathbb{R}$  is then sampled from a Gaussian distribution  $P(x | y) = \mathcal{N}(m_y, s_y)$  with mean  $m_y$  and scale  $s_y$  dependent of  $y$ . We set  $m_y = (2 \times y - 1)$  and  $s_y = 2$ , and change the parameter  $\pi$  for each setting below. By Bayes’ theorem, the conditional probability of  $y$  given  $x$  corresponds to a logistic model:  $P(y | x) = 1/(1 + \exp(\beta_0 + \beta_1 \times x))$  where  $\beta_0 = \log(\pi/(1 - \pi))$  and  $\beta_1 = 4$ . A logistic model is therefore capable of reproducing the probability  $P(y | x)$  of this synthetic data perfectly.

We consider two baseline cases of (i) well-balanced classification and (ii) imbalanced classification in this experiment. We train a logistic model for the training data simulated with the parameter  $\pi = 0.5$  (i.e. 50% prevalence) in case (i) and

with  $\pi = 0.01$  (i.e. 1% prevalence) in case (ii). In each case (i) and (ii), we generate three different test datasets to create situations where the trained model is (a) well-calibrated, (b) over-calibrated, and (c) under-calibrated. We examine the performance of TCE under these scenarios. Test datasets for scenarios (a), (b), and (c) are generated from the simulation model with prevalences 50%, 40%, and 60% in case (i) and with prevalences 1%, 0%, and 2% in case (ii). We generate 20000 data points in total, of which 70% are training data and 30% are test data.

Table 2 shows the values of four calibration error metrics applied to the logistic regression model in each scenario. Table 2 demonstrates that all values of ECE and ACE in imbalanced case (ii) can be smaller than—or very close to—values for well-calibrated scenario (a) in well-balanced case (i). For example, the ECE value for case (ii)-(b) was smaller than that for case (i)-(a). In contrast, TCE provides values with a consistent scale in both well-balanced and imbalanced cases. More simulation studies of TCE with different hyperparameters are presented in Appendix C.1.

Table 2: Comparison of four calibration error metrics under scenarios (a) - (c) in each case (i) and (ii).

Prevalence	TCE	TCE(Q)	ECE	ACE
50% vs 50%	7.28%	10.88%	0.0138	0.0150
50% vs 40%	96.10%	96.47%	0.0963	0.0951
50% vs 60%	98.83%	98.93%	0.1097	0.1096
1% vs 1%	3.40%	0.18%	0.0017	0.0031
1% vs 0%	95.50%	68.73%	0.0094	0.0094
1% vs 2%	92.32%	89.73%	0.0139	0.0139

## 4.2 IMBALANCED UCI DATASETS

Next, we compare calibration error metrics using real-world datasets in the regime of severe class imbalance. We use nine UCI datasets that were preprocessed by Lemaître et al. [2017] as benchmark tasks of imbalanced classification. We also use one additional UCI dataset with a well-balanced prevalence for comparison. For each dataset, 70% of samples are used as training data and 30% of samples are kept as validation data. We train five different algorithms: logistic regression (LR), support vector machine (SVM), random forest (RF), gradient boosting (GB), and multi-layer perceptron (MLP). We evaluate the calibration performance of each model by five different calibration error metrics in the following tables. Tables 3 and 4 show results for the imbalanced datasets, *abalone* and *webpage* [Dua and Graff, 2017], respectively. Results for all the other datasets are presented in Appendix C.2. In Table 3, the best model ranked by TCE and ACE agree with each other while ECE identifies RF as the best model. It can be observed from the reliability diagram of ECE for both the datasets in Appendix C.2 that

a large majority of model predictions are contained in a single bin of ECE. In such cases, ECE becomes essentially equivalent to a comparison of global averages of all labels and all model predictions. Table 4 demonstrates a situation where ECE and ACE risk misleading assessments of calibration performance. Several values of ECE and ACE are all sufficiently small in Table 4, by which one may conclude that it is reasonable to use a model with the smallest calibration error. However, the values of TCE indicate that no model has a good calibration performance. In fact, relatively large statistical deviations between model predictions and empirical probabilities can be observed from the test-based reliability diagram for the webpage dataset in Appendix C.2.

Table 3: Comparison of five calibration error metrics for five different algorithms trained on the abalone dataset.

	TCE	ECE	ACE	MCE	MCE(Q)
LR	7.26%	0.0140	0.0252	0.0946	0.0851
SVM	47.21%	0.0436	0.0473	0.8302	0.1170
RF	33.89%	0.0127	0.0177	0.0670	0.0547
GB	4.86%	0.0182	0.0160	0.2965	0.0418
MLP	3.83%	0.0167	0.0122	0.0806	0.0540

Table 4: Comparison of five calibration error metrics for five different algorithms trained on the webpage dataset.

	TCE	ECE	ACE	MCE	MCE(Q)
LR	40.16%	0.0044	0.0034	0.3134	0.0214
SVM	59.83%	0.0043	0.0057	0.5402	0.0239
RF	99.66%	0.0234	0.0241	0.5980	0.1189
GB	71.12%	0.0086	0.0107	0.2399	0.0436
MLP	49.81%	0.0090	0.0018	0.4344	0.0076

## 4.3 K-VS-REST ON IMAGENET1000

Finally, we demonstrate that TCE is applicable for a large-scale binary classification task using ImageNet1000 data. We consider a K-vs-rest classification problem by using a set of all dog-kind classes (from class 150 to class 275) as a positive class and the rest as a negative class. Under this setting, 12.5% of validation samples belong to the positive class. We used 5 different trained models: AlexNet, VGG19, ResNet18, ResNet50, and ResNet152. Their calibration errors were measured based on the ImageNet1000 validation dataset consisting of 50000 data points. Table 5 demonstrates that TCE produces interpretable values, with model rankings that largely agree with other metrics in this setting. The last row of Table 5 shows the average computational time of each metric. Computation of all the procedures in TCE required only 71.78 seconds for 50000 data points with 1 CPU on average. The reliability diagrams corresponding to the results are presented in Appendix C.3.

Table 5: Comparison of five calibration error metrics for five different deep learning models on ImageNet1000 data.

	TCE	ECE	ACE	MCE	MCE(Q)
AlexNet	42.74%	0.0070	0.0070	0.1496	0.0528
VGG19	23.57%	0.0028	0.0028	0.2148	0.0247
Res18	29.93%	0.0042	0.0042	0.2368	0.0350
Res50	24.60%	0.0020	0.0018	0.1911	0.0152
Res152	16.09%	0.0012	0.0013	0.1882	0.0102
<b>Time (s)</b>	71.78	0.4873	0.4221	0.0046	0.0063

## 5 RELATED WORK

Several calibration error metrics have been proposed, including the aforementioned ECE. MCE is a widely used variant of ECE that replaces the summation over  $b = 1, \dots, B$  in (4) with the supremum over  $b = 1, \dots, B$ . [Kumar et al., 2019] introduce a more general  $l_p$  calibration error, which includes both ECE and MCE. ACE replaces the equispaced bins in ECE with bins designed based on quantiles of model predictions, which prevents high concentration of data in one bin when data is imbalanced [Nixon et al., 2019]. These calibration error metrics can be extended to multi-class classification [Kumar et al., 2019]. Other than calibration error, scoring functions [Gneiting et al., 2007] are commonly used measurements to evaluate a probabilistic classifier. [Wallace and Dahabreh, 2014] reported a limitation of the Brier score for imbalanced classification, and proposed the *stratified* Brier score that aggregates multiple Brier scores.

This paper designed a new calibration error metric based on a statistical test. While statistical tests have been used in the context of calibration, we are the first to incorporate a statistical test into the design of a calibration error metric. Vaicenavicius et al. [2019] performed a statistical test on whether ECE computed for synthetic data generated from predictive probabilities is significantly different from ECE computed for actual data. Similarly, Widmann et al. [2019] proposed a statistical test of the value of their calibration error metric built on kernel methods. In contrast to existing works which considered a test for final values of calibration error metrics, our approach incorporates a test into the metric itself.

While the use of binning is vital in the vast majority of calibration metrics, there are a few works on the *binning-free* design of calibration error metrics. The main idea is to use an cumulative distribution function (CDF) of predictive probabilities, which can be estimated without binning, and evaluate how significantly it differs from an ideal CDF that occurs if the predictive probabilities are all well-calibrated. For example, Gupta et al. [2021] and Arrieta-Ibarra et al. [2022] considered the Kolmogorov-Smirnov test for the empirical CDF, where Gupta et al. [2021] further proposed a spline interpolation to obtain a continuous approximation

of the CDF. An approach proposed by Kull et al. [2017] can also be regarded as binning-free. It uses a continuous CDF of the beta distribution produced by their calibration method, mentioned below, rather than the empirical CDF.

*Calibration methods* refer to algorithms used to improve the calibration performance of a model  $P_\theta$ . Usually, they learn some ‘post-hoc’ function  $\varphi : [0, 1] \rightarrow [0, 1]$  to be applied to each model prediction so that the new prediction  $\varphi(P_\theta(x))$  is better calibrated. Various calibration algorithms have been proposed in parallel to the development of calibration error metrics. Platt scaling uses a logistic function for the post-hoc function  $\varphi$  [Platt, 1999]. Alternatively, Kull et al. [2017, 2019] proposed to use a beta distribution in binary classification and a Dirichlet distribution in multi-class classification. Isotonic regression is a powerful non-parametric approach to find a monotonically increasing function  $\varphi$  that minimises the Brier score [Zadrozny and Elkan, 2002]. Finally, Bayesian Binning into Quantiles by Naeini et al. [2015] extends a classical histogram-based calibration [Zadrozny and Elkan, 2001] to an ensemble of histogram-based calibrations based on Bayesian model averaging.

## 6 CONCLUSION

In this paper, we proposed a new calibration error metric TCE that incorporates a novel loss function based on a statistical test. TCE has (i) a clear interpretation as a percentage of model predictions determined to deviate significantly from estimated empirical probabilities, (ii) a consistent scale that is robust to class imbalance, and (iii) an informative visual representation that facilitates a better understanding of calibration performance of probabilistic classifiers. We further introduced an optimality criterion of bins associated with a minimal estimation error of the empirical probabilities and a new algorithm to compute optimal bins approximately under the constraint of the size of each bin.

Our proposal opens up room for new research directions in the context of calibration. This paper focuses on the methodological development of TCE. There are various directions to investigate in terms of theoretical properties of TCE. These include the convergence properties of TCE in the limit of data size  $N$ , understanding the minimum number of data points that should be contained in each subset  $\mathcal{D}_b$ , and a rigorous theoretical analysis of PAVA-BC. By continuing to investigate these areas, we can refine and expand our understanding of the capabilities of TCE.

## Acknowledgements

The authors would like to thank Abbas Zaidi, Michael Gill, and Will Bullock for their useful feedback on early work of this paper. TM is supported by The Alan Turing Institute under the EPSRC grant EP/N510129/1.

## References

- Aisha Abdallah, Mohd Aizaini Maarof, and Anazida Zainal. Fraud detection system: A survey. *Journal of Network and Computer Applications*, 68:90–113, 2016. ISSN 1084-8045.
- Imanol Arrieta-Ibarra, Paman Gujral, Jonathan Tannen, Mark Tygert, and Cherie Xu. Metrics of calibration for probabilistic predictions. *Journal of Machine Learning Research*, 23(351):1–54, 2022.
- Ralf Bender and Stefan Lange. Adjusting for multiple testing—when and how? *Journal of Clinical Epidemiology*, 54(4):343–349, 2001. ISSN 0895-4356.
- Glen W. Brier. Verification of forecasts expressed in terms of probability. *Monthly Weather Review*, 78(1):1 – 3, 1950.
- Jochen Bröcker. Reliability, sufficiency, and the decomposition of proper scores. *Quarterly Journal of the Royal Meteorological Society*, 135(643):1512–1519, 2009.
- Philip Dawid. The well-calibrated bayesian. *Journal of the American Statistical Association*, 77(379):605–610, 1982.
- Jan de Leeuw, Kurt Hornik, and Patrick Mair. Isotone optimization in r: Pool-adjacent-violators algorithm (pava) and active set methods. *Journal of Statistical Software*, 32(5):1–24, 2009.
- Morris H. Degroot and Stephen E. Fienberg. The comparison and evaluation of forecasters. *The Statistician*, 32: 12–22, 1983.
- Timo Dimitriadis, Tilmann Gneiting, and Alexander I. Jordan. Stable reliability diagrams for probabilistic classifiers. *Proceedings of the National Academy of Sciences*, 118(8), 2021.
- Dheeru Dua and Casey Graff. UCI machine learning repository, 2017. URL <http://archive.ics.uci.edu/ml>.
- M Elter, R Schulz-Wendtland, and T Wittenberg. The prediction of breast cancer biopsy outcomes using two cad approaches that both emphasize an intelligible decision process. *Medical Physics*, 34(11), 2007.
- Tilmann Gneiting, Fadoua Balabdaoui, and Adrian E. Raftery. Probabilistic forecasts, calibration and sharpness. *Journal of the Royal Statistical Society: Series B (Statistical Methodology)*, 69(2):243–268, 2007.
- Sorin Grigorescu, Bogdan Trasnea, Tiberiu Cocias, and Gigel Macesanu. A survey of deep learning techniques for autonomous driving. *Journal of Field Robotics*, 37(3): 362–386, 2020.
- Kartik Gupta, Amir Rahimi, Thalaiyasingam Ajanthan, Thomas Mensink, Cristian Sminchisescu, and Richard Hartley. Calibration of neural networks using splines. In *International Conference on Learning Representations*, 2021.
- Alexander Henzi, Alexandre Mösching, and Lutz Dümbgen. Accelerating the Pool-Adjacent-Violators Algorithm for Isotonic Distributional Regression. *Methodology and Computing in Applied Probability*, 24(4):2633–2645, 2022.
- Meelis Kull, Telmo M. Silva Filho, and Peter Flach. Beyond sigmoids: How to obtain well-calibrated probabilities from binary classifiers with beta calibration. *Electronic Journal of Statistics*, 11(2):5052 – 5080, 2017.
- Meelis Kull, Miquel Perello Nieto, Markus Kängsepp, Telmo Silva Filho, Hao Song, and Peter Flach. Beyond temperature scaling: Obtaining well-calibrated multi-class probabilities with dirichlet calibration. In *Advances in Neural Information Processing Systems*, volume 32, 2019.
- Ananya Kumar, Percy S Liang, and Tengyu Ma. Verified uncertainty calibration. In *Advances in Neural Information Processing Systems*, volume 32, 2019.
- Guillaume Lemaître, Fernando Nogueira, and Christos K. Aridas. Imbalanced-learn: A python toolbox to tackle the curse of imbalanced datasets in machine learning. *Journal of Machine Learning Research*, 18(17):1–5, 2017.
- Cheng Li, Yue Lu, Qiaozhu Mei, Dong Wang, and Sandeep Pandey. Click-through prediction for advertising in twitter timeline. In *Proceedings of the 21th ACM SIGKDD International Conference on Knowledge Discovery and Data Mining*, pages 1959–1968, 2015.
- Matthias Minderer, Josip Djolonga, Rob Romijnders, Frances Ann Hubis, Xiaohua Zhai, Neil Houlsby, Dustin Tran, and Mario Lucic. Revisiting the calibration of modern neural networks. In *Advances in Neural Information Processing Systems*, 2021.
- M. P. Naeini, G. F. Cooper, and M. Hauskrecht. Obtaining well calibrated probabilities using bayesian binning. In *Proceedings of the AAAI Conference on Artificial Intelligence*, pages 2901—2907, 2015.
- Alexandru Niculescu-Mizil and Rich Caruana. Predicting good probabilities with supervised learning. In *Proceedings of the 22nd International Conference on Machine Learning*, page 625–632, 2005.
- Jeremy Nixon, Michael W. Dusenberry, Linchuan Zhang, Ghassen Jerfel, and Dustin Tran. Measuring calibration in deep learning. In *Proceedings of the IEEE/CVF Conference on Computer Vision and Pattern Recognition (CVPR) Workshops*, June 2019.

- John C. Platt. Probabilistic outputs for support vector machines and comparisons to regularized likelihood methods. *Advances in Large Margin Classifiers*, 10(3), 1999.
- Amos Storkey et al. When training and test sets are different: characterizing learning transfer. *Dataset shift in machine learning*, 30:3–28, 2009.
- Niek Tax, Kees Jan de Vries, Mathijs de Jong, Nikoleta Dosoula, Bram van den Akker, Jon Smith, Olivier Thuong, and Lucas Bernardi. Machine learning for fraud detection in e-commerce: A research agenda. In *Proceedings of the KDD International Workshop on Deployable Machine Learning for Security Defense (MLHat)*, pages 30–54. Springer, 2021.
- Ryan J. Tibshirani, Holger Hoefling, and Robert Tibshirani. Nearly-isotonic regression. *Technometrics*, 53(1):54–61, 2011.
- Eric Topol. High-performance medicine: the convergence of human and artificial intelligence. *Nature Medicine*, 25: 44–56, 2019.
- Juozas Vaicenavicius, David Widmann, Carl R. Andersson, Fredrik Lindsten, Jacob Roll, and Thomas Bo Schön. Evaluating model calibration in classification. In *Proceedings of the 22nd International Conference on Artificial Intelligence and Statistics*, 2019.
- Peter van der Putten and Maarten van Someren. Coil challenge 2000: The insurance company case. Technical report, Sentient Machine Research, Amsterdam and Leiden Institute of Advanced Computer Science, 2000-2009.
- Byron C Wallace and Issa J Dahabreh. Improving class probability estimates for imbalanced data. *Knowledge and Information Systems*, 41(1):33–52, 2014.
- David Widmann, Fredrik Lindsten, and Dave Zachariah. Calibration tests in multi-class classification: A unifying framework. In *Advances in Neural Information Processing Systems*, volume 32, 2019.
- Yanwu Yang and Panyu Zhai. Click-through rate prediction in online advertising: A literature review. *Information Processing & Management*, 59(2):102853, 2022.
- Bianca Zadrozny and Charles Elkan. Obtaining calibrated probability estimates from decision trees and naive bayesian classifiers. In *Proceedings of the Eighteenth International Conference on Machine Learning*, page 609–616, 2001.
- Bianca Zadrozny and Charles Elkan. Transforming classifier scores into accurate multiclass probability estimates. In *Proceedings of the Eighth ACM SIGKDD International Conference on Knowledge Discovery and Data Mining*, page 694–699, 2002.

---

# TCE: A Test-Based Approach to Measuring Calibration Error (Supplementary Material)

---

Takuo Matsubara<sup>1,2</sup>

Niek Tax<sup>3</sup>

Richard Mudd<sup>3</sup>

Ido Guy<sup>3</sup>

<sup>1</sup>The Alan Turing Institute

<sup>2</sup>Newcastle University

<sup>3</sup>Meta Platforms, Inc.

This supplement contains all the additional results referred to in the main text. Appendix A contains the proof that the optimisation criterion of eq. (8) is indeed minimised using PAVA. Appendix B shows an example of bins obtained using PAVA-BC that caused mild violation of the monotonic constraint of the empirical probabilities  $\{\hat{P}_b\}_{b=1}^B$ . Finally, additional experimental results are presented in Appendix C.

## A OPTIMAL BINS BASED ON PAVA

The optimal bins defined by Definition 3 can be exactly computed under the error function D specified by eq. (9) which corresponds to the variance of each  $\mathcal{D}_b^y$ . The optimal bins result in minimisation of a weighted average of the variance of each  $\mathcal{D}_b^y$  over all  $b$ , where the weights are proportional to the size of each bin. The following proposition shows that Algorithm 3 with PAVA-BC replaced by PAVA generates the optimal bins under the error function D. In what follows, we assume a standard setting where the solution of eq. (8) is at least not a set of only one single bin, i.e.,  $\{\Delta_b\}_{b=1}^1 = \{[0, 1]\}$ .

**Proposition 1.** *The minimum of eq. (8) in Definition 3 under the error function D in eq. (9) is attained at bins computed by Algorithm 3 with PAVA-BC replaced by PAVA.*

*Proof.* First, we show that the optimisation problem of eq. (8) in Definition 3 under the loss function D in eq. (9) is equivalent to the monotonic regression problem under the squared error. Recall that, given a choice of bins  $\{\Delta_b\}_{b=1}^B$ , each label subset  $\mathcal{D}_b^y$  is defined by  $\mathcal{D}_b^y := \{y_i \in \mathcal{D}^y \mid P_\theta(x_i) \in \Delta_b\}$ . The input of Algorithm 3 is a set of labels  $\mathcal{D}^y = \{y_i\}_{i=1}^N$  ordered by in ascending order of  $\{P_\theta(x_i)\}_{i=1}^N$ . This means that each label subset  $\mathcal{D}_b^y$  is a set of consecutive elements in the ordered set  $\{y_i\}_{i=1}^N$ . Therefore, there exist corresponding indices  $n_b$  and  $n_{b+1}$  s.t. each label subset  $\mathcal{D}_b^y$  can be expressed by

$$\mathcal{D}_b^y = \{y_i \in \mathcal{D}^y \mid P_\theta(x_i) \in \Delta_b\} = \{y_i \in \mathcal{D}^y \mid i \text{ s.t. } n_b \leq i < n_{b+1}\}.$$

Accordingly, with the ordered labels  $\mathcal{D}^y$ , each empirical probability  $\hat{P}_b$  in  $\mathcal{D}_b^y$  can be expressed by

$$\hat{P}_b = \frac{1}{N_b} \sum_{y \in \mathcal{D}_b^y} y = \frac{1}{n_{b+1} - n_b} \sum_{j=n_b}^{n_{b+1}-1} y_j.$$

Define a set of scalars  $\{g_i\}_{i=1}^N$  whose element  $g_i \in [0, 1]$  corresponds to the empirical probability  $\hat{P}_b$  of the bin index  $b$  if  $n_b \leq i < n_{b+1}$ . Namely,

$$g_i := \hat{P}_b = \frac{1}{n_{b+1} - n_b} \sum_{j=n_b}^{n_{b+1}-1} y_j \quad \text{for each } i \text{ s.t. } n_b \leq i < n_{b+1}. \quad (10)$$

Under these notations, the optimisation criterion in eq. (8) can be rewritten as

$$\sum_{b=1}^B W_b \times D(\mathcal{D}_b, \hat{P}_b) = \frac{1}{N} \sum_{b=1}^B \sum_{y \in \mathcal{D}_b} (y - \hat{P}_b)^2 = \frac{1}{N} \sum_{b=1}^B \sum_{i=n_b}^{n_{b+1}-1} (y_i - \hat{P}_b)^2 = \frac{1}{N} \sum_{i=1}^N (y_i - g_i)^2. \quad (11)$$

This formulation translates a problem of choosing bins  $\{\Delta_b\}_{b=1}^B$  into a problem of finding a monotonically increasing sequence  $\{g_i\}_{i=1}^N$  that is determined by the choice of indices  $\{n_b\}_{b=1}^B$ , so that eq. (11) is minimised. Therefore the optimisation problem of eq. (8) in Definition 3 under the loss function  $D$  in eq. (9) is equivalent to the monotonic regression problem under the squared error whose solution sequence  $\{g_i\}_{i=1}^N$  is restricted to a form of eq. (10).

Next, consider a standard monotonic regression problem under the square error  $\sum_{i=1}^N (y_i - \hat{y}_i)^2$  for the ordered set  $\{y_i\}_{i=1}^N$ . PAVA finds a monotonically increasing sequence  $\{\hat{y}_i\}_{i=1}^N$  that minimises the square error. The solution sequence  $\{\hat{y}_i\}_{i=1}^N$  by PAVA is given in a form of eq. (10); see e.g. [de Leeuw et al., 2009, Henzi et al., 2022]. This means that there exists a set of indices  $\{n_b^*\}_{b=1}^B$  s.t. the solution sequence  $\{\hat{y}_i\}_{i=1}^N$  by PAVA is expressed as

$$\hat{y}_i = \frac{1}{n_{b+1}^* - n_b^*} \sum_{j=n_b^*}^{n_{b+1}^*} y_j \quad \text{for each } i \quad \text{s.t.} \quad n_b^* \leq i < n_{b+1}^*$$

and the sequence  $\{\hat{y}_i\}_{i=1}^N$  satisfies the monotonic constraint  $\hat{y}_1 \leq \dots \leq \hat{y}_N$  holds. We can obtain such a solution sequence  $\{\hat{y}_i\}_{i=1}^N$  by applying any standard implementation of PAVA.

An output of most implementations of PAVA is the solution sequence  $\{\hat{y}_i\}_{i=1}^N$  rather than the associated indices  $\{n_b^*\}_{b=1}^B$ . However, the indices  $\{n_b^*\}_{b=1}^B$  can be easily recovered from a given solution sequence  $\{\hat{y}_i\}_{i=1}^N$  of PAVA by simply finding all indices  $i$  s.t.  $\hat{y}_i \neq \hat{y}_{i+1}$ . Finally, we consider constructing bins  $\{\Delta_b\}_{b=1}^B$  based on the recovered indices  $\{n_b^*\}_{b=1}^B$ . Recall that the set of labels  $\mathcal{D}^y = \{y_i\}_{i=1}^N$  are ordered in ascending order of  $\{P_\theta(x_i)\}_{i=1}^N$ . If we construct each bin  $\Delta_b$  by

$$\Delta_b := \left[ \frac{P_\theta(x_{n_b^*-1}) + P_\theta(x_{n_b^*})}{2}, \frac{P_\theta(x_{n_{b+1}^*-1}) + P_\theta(x_{n_{b+1}^*})}{2} \right],$$

it is sufficient to generate each label subset  $\mathcal{D}_b^y$  that corresponds to

$$\mathcal{D}_b^y = \{y_i \in \mathcal{D}^y \mid P_\theta(x_i) \in \Delta_b\} = \{y_i \in \mathcal{D}^y \mid i \text{ s.t. } n_b^* \leq i < n_{b+1}^*\}.$$

Then the optimisation criterion in eq. (8), which is translated to the error of the monotonic regression problem of PAVA, is minimised by the choice of bins produced in this procedure. Observing that Algorithm 3 with PAVA-BC replaced by PAVA performs this procedure concludes the proof.  $\square$

## B MILD VIOLATION OF MONOTONICITY BY PAVA-BC

A monotonic regression algorithm finds a monotonically increasing sequence  $\hat{y}_1 \leq \dots \leq \hat{y}_N$  that minimises some error  $D(\{\hat{y}_i\}_{i=1}^N, \{y_i\}_{i=1}^N)$  for a given ordered set  $\{y_i\}_{i=1}^N$ . PAVA is one of the most common monotonic regression algorithms that uses the square error  $\sum_{i=1}^N (\hat{y}_i - y_i)^2$ . For some partition  $\mathcal{A}$  of indices  $I = \{1, \dots, N\}$  whose element  $A \in \mathcal{A}$  is a set of consecutive indices in  $I$ , PAVA produces a solution sequence s.t. each element  $\hat{y}_i$  is given by  $\hat{y}_i = (1/|A|) \sum_{i \in A} y_i$  for  $A$  in which  $i \in A$ . We refer to each element  $A$  in the partition  $\mathcal{A}$  of indices  $I$  as *block*. PAVA-BC produces a solution sequence that approximates the solution sequence by PAVA under the constraints of the minimum and maximum size of each block. For some partition  $\mathcal{A}'$  of indices  $I$ , each element  $\hat{y}_i$  of the solution sequence is given by  $\hat{y}_i = (1/|A'|) \sum_{i \in A'} y_i$  for  $A'$  in which  $i \in A'$  in the same manner as PAVA. PAVA-BC meets the minimum and maximum size constraints of each block  $A' \in \mathcal{A}'$  at the cost of the possibility of mild violation of the monotonic constraint. It depends on the minimum and maximum size constraints, data, and models whether violation of the monotonic constraint occurs by PAVA-BC. Figure 3 shows an example where bins based on PAVA-BC did not violate the monotonicity of the empirical probabilities  $\{\hat{P}_b\}_{b=1}^B$ . Figure 3 was computed using a random forest model trained on the *satimage* dataset used in Section 4.2, and corresponds to Figure 2 presented in Section 3. The total estimation error in eq. (8) and an average of the estimation error within each bin in eq. (9) for each set of the bins in Figure 3 were summarised in Table 1 presented in Section 3. Figure 4 shows an example where bins based on PAVA-BC violated the monotonic constraint of the empirical probabilities  $\{\hat{P}_b\}_{b=1}^B$ . Figure 4 was computed using a random forest model trained on the *coil\_2000* dataset used in Section 4.2. The total estimation error in eq. (8) for each set of the bins in Figure 4 was 0.0509, 0.0517, and 0.0521 for PAVA, PAVA-BC, binning based on 10-quantiles, respectively. An average of the estimation error within each bin in eq. (9) for each set of the bins in Figure 3 was 0.0834, 0.0627, and 0.0520 for PAVA, PAVA-BC, binning based on 10-quantiles, respectively.

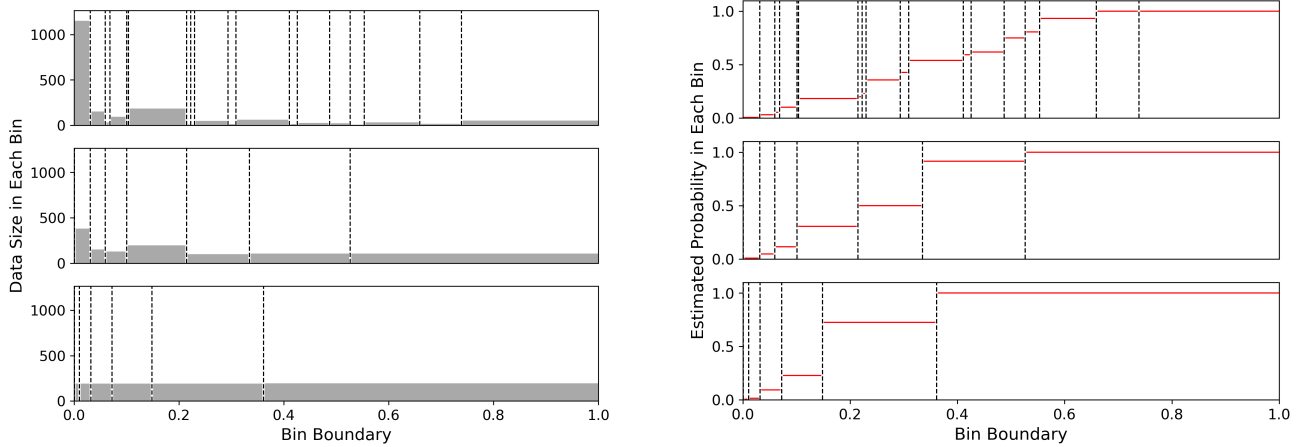


Figure 3: Comparison of bins based on three different approaches for a random forest model on the satimage dataset: (top) PAVA, (middle) PAVA-BC, (bottom) binning based on 10-quantiles. The dotted line in the left and right panels represents the boundary of each bin. The grey bar in the left panel represents the size of each bin. The red line in the right panel represents the empirical probability of each bin.

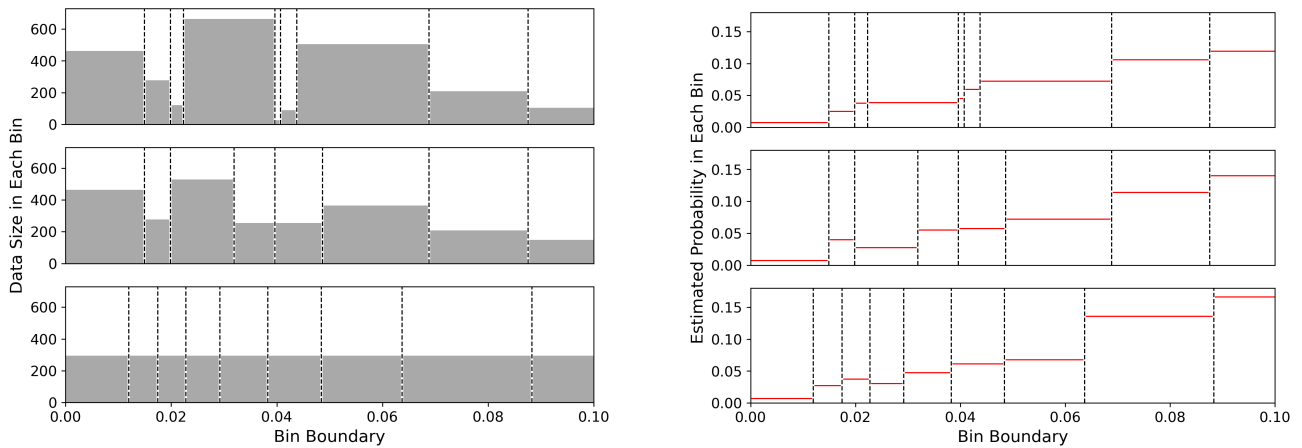


Figure 4: Comparison of bins based on three different approaches for a random forest model on the satimage dataset: (top) PAVA, (middle) PAVA-BC, (bottom) binning based on 10-quantiles. Each axis is restricted to a range  $[0.0, 0.1]$  as the majority of bins were contained in the range in this example. The dotted line in the left and right panels represents the boundary of each bin. The grey bar in the left panel represents the size of each bin. The red line in the right panel represents the empirical probability of each bin. A random forest model trained on the coil\_2000 dataset was used.

## C ADDITIONAL EXPERIMENTS

We present additional experiments in each section that complement the experiments illustrated in the main text. We use the same settings as the main text for the minimum and maximum size for bins based on PAVA-BC as well as the bin number  $B$  for equi-spaced and quantile-based bins.

### C.1 SIMULATION STUDY OF TCE

We perform detailed simulation studies of TCE in the same simplified setting as Section 4.1. We demonstrate sensitivity of TCE to its hyperparameters, an impact of different dataset size and prevalence, and sensitivity to a small perturbation to model predictions. In all experiments, we generated training and test data from the Gaussian discriminant analysis in Section 4.1, each with the prevalence  $P_{\text{training}}(y)$  and  $P_{\text{test}}(y)$ , and compute TCE of a logistic model fitted to the training data. In all experiments except ones on an impact of different dataset size and prevalence, we set the training data size to 14000 and set the test data size to 6000. We then examine two cases where the model is calibrated and miscalibrated synthetically, setting  $P_{\text{training}}(y) = 0.5$  and  $P_{\text{test}}(y) = 0.5$  for the first case and setting  $P_{\text{training}}(y) = 0.5$  and  $P_{\text{test}}(y) = 0.4$  for the second case. In summary, we present the following experimental analyses:

- Sensitivity to the minimum bin size  $N_{\min}$  in PAVA-BC from  $N_{\min} = 1$  to  $N_{\min} = 3000$ ;
- Sensitivity to the maximum bin size  $N_{\max}$  in PAVA-BC from  $N_{\max} = 6$  to  $N_{\max} = 6000$ ;
- Sensitivity to a pair of  $(N_{\min}, N_{\max})$  in PAVA-BC chosen so that each binsize fall into selected ranges;
- Sensitivity to a small perturbation of predictions by a logit-normal noise with scale  $\sigma$  from  $\sigma = 0.0$  to  $\sigma = 1.0$ ;
- Sensitivity to a choice of significance level  $\alpha$  in the Binomial test from  $\alpha = 0.0001$  to  $\alpha = 0.1$ ;
- Comparison of TCE by different choices of test, binomial test and t-test;
- Comparison of TCE by different total sizes  $N$  of test dataset from  $N = 30$  to  $N = 60000$ ;
- Comparison of TCE by different prevalences  $P$  of dataset from  $P = 0.5$  to  $P = 0.02$ .

Tables 6 to 13 presents the result of each experiment above in order. In each table, TCE(P) denotes TCE based on PAVA-BC, TCE(Q) denotes TCE based on quantile-binning, and TCE(V) denotes TCE based on PAVA. For reference, we include values of ECE, ACE, MCE, and MCE(Q), where MCE(Q) denotes MCE based on quantile-binning. Observations from each result in are summarised as follows.

- Table 6: The performance of TCE(P) to evidence the well-calibrated model was consistently reasonable for any minimum binsize constant between  $N_{\max} = 1$  and  $N_{\max} = 600$ , while there was a breakdown point between  $N_{\min} = 600$  and  $N_{\min} = 3000$  where TCE(P) was no longer able to do so. This is likely because the number of bins produced under the constraint  $N_{\min} = 3000$  for the total datasize 6000 was 2 at maximum, which was too small to estimate the empirical probabilities  $\{\hat{P}_b\}_{b=1}^B$  accurately.
- Table 7: The performance of TCE(P) to evidence the miscalibrated model was consistently reasonable for any maximum binsize constant between  $N_{\max} = 300$  and  $N_{\max} = 6000$ , while there was a breakdown point between  $N_{\min} = 60$  and  $N_{\min} = 300$  where TCE(P) was no longer able to do so. This is likely because the number of bins produced under the constraint  $N_{\max} = 60$  for the total datasize 6000 was 100 at minimum, which is too large to estimate the empirical probabilities  $\{\hat{P}_b\}_{b=1}^B$  accurately.
- Table 8: The performance of TCE(P) to evidence both the well-calibrated and miscalibrated models was arguably the most reasonable when  $(N_{\min}, N_{\max})$  was chosen so that the number of bins produced falls into the range  $[5, 20]$ . This suggests a heuristic to use such  $(N_{\min}, N_{\max})$  for other experiments.
- Table 9: At each model prediction  $P_\theta(x)$ , we sample a new prediction from a logit-normal distribution centred at  $P_\theta(x)$  with scale  $\sigma$  to generate a perturbed prediction by a small noise. All calibration error metrics were shown to have similar sensitivities to the noise. The scale between  $\sigma = 0.10$  and  $\sigma = 0.50$  was the breakdown point where each metric started to produce an unreasonable score for the well-calibrated model.
- Table 10: The performance of TCE(P) to evidence both the well-calibrated and miscalibrated models was consistently reasonable for any significant level between  $\alpha = 0.001$  and  $\alpha = 0.1$ , while there was a breakdown point between  $\alpha = 0.1$  and  $\alpha = 0.5$  where TCE(P) was no longer able to do so for the well-calibrated model.

- Table 11: TCE based on the Binomial test outperformed one based on the t-test in the majority of the settings. It is possible that the Binomial test produces more accurate outcomes than the t-test, given that it is an exact test whose test statistics does not involve any approximation.
- Table 12: The performance of TCE(P) to evidence both the well-calibrated and miscalibrated models was consistently reasonable for any dataset size between  $N_{\text{test}} = 3000$  and  $N_{\text{test}} = 60000$ , while there was a breakdown point between  $N_{\text{test}} = 600$  and  $N_{\text{test}} = 3000$  where TCE(P) was no longer able to do so for the well-calibrated model. This is likely because the dataset size  $N_{\text{test}} = 600$  was not big enough to estimate the empirical probabilities  $\{\hat{P}_b\}_{b=1}^B$  accurately. This result may be improved by using different settings of the minimum and maximum binsize constraints.
- Table 13: The performance of TCE(P) on both the well-calibrated and miscalibrated models was reasonable for any prevalence. While there was a fluctuation in values of TCE(P) for different values of prevalence, TCE(P) overall produced better values than TCE(Q) and TCE(V).

Table 6: Sensitivity to the minimum binsize  $N_{\text{min}} = 1, 6, 30, 300, 600, 3000$  in PAVA-BC. For comparison purpose, the number of bins  $B$  of quantile-binning and equispaced-binning was varied as  $B = 1000, 500, 100, 50, 10, 5, 1$  along with  $N_{\text{min}}$ . Note that TCE(V) is a constant across all the row because PAVA does not involve any binsize constraint.

Test Prevalence	Min Binsize	TCE(P)	TCE(Q)	TCE(V)	ECE	ACE	MCE	MCE(Q)
50% (Calibrated)	1	3.4500	5.1000	3.4500	0.1143	0.1651	0.8767	0.6392
	6	3.3833	4.2000	3.4500	0.0839	0.1142	0.8767	0.5016
	30	2.3500	4.3000	3.4500	0.0382	0.0457	0.8767	0.1705
	60	2.6333	3.5667	3.4500	0.0271	0.0370	0.2533	0.1189
	300	7.2833	10.8833	3.4500	0.0138	0.0150	0.1020	0.0528
	600	13.5667	38.7500	3.4500	0.0116	0.0086	0.1020	0.0236
	3000	92.2000	92.2000	3.4500	0.0021	0.0021	0.0021	0.0021
40% (Miscalibrated)	1	88.0667	6.6667	88.0667	0.1417	0.1847	0.8767	0.6111
	6	88.0667	8.7000	88.0667	0.1179	0.1389	0.8767	0.4811
	30	88.3333	32.2833	88.0667	0.0993	0.0992	0.8767	0.2264
	60	87.8667	56.7667	88.0667	0.0971	0.0964	0.2426	0.1827
	300	96.1000	96.4667	88.0667	0.0963	0.0951	0.1466	0.1314
	600	96.6000	96.7833	88.0667	0.0963	0.0951	0.1099	0.1092
	3000	93.9500	93.9500	88.0667	0.0951	0.0951	0.0951	0.0951



Table 9: Sensitivity to a small perturbation to model predictions by a logit-normal noise with scale  $\sigma = 0.01, 0.05, 0.10, 0.50, 1.00$ . The maximum and minimum binsize of PAVA-BC were set to 1200 and 300. The number of bins of quantile-binning and equispaced-binning was set 10.

Test Prevalence	Noise Level	TCE(P)	TCE(Q)	TCE(V)	ECE	ACE	MCE	MCE(Q)
50% (Calibrated)	0.00	7.2833	10.8833	3.4500	0.0138	0.0150	0.1020	0.0528
	0.01	8.7167	9.6167	4.8000	0.0113	0.0125	0.0923	0.0527
	0.05	12.8833	11.9000	7.7667	0.0136	0.0156	0.1198	0.0589
	0.10	8.3500	13.0500	3.5500	0.0109	0.0164	0.1143	0.0587
	0.50	61.9500	65.0500	56.1000	0.0615	0.0618	0.3601	0.1498
	1.00	86.1833	84.1000	88.3833	0.1470	0.1478	0.3364	0.2621
40% (Miscalibrated)	0.00	96.1000	96.4667	88.0667	0.0963	0.0951	0.1466	0.1314
	0.01	96.4000	96.4000	89.6167	0.0962	0.0951	0.1511	0.1332
	0.05	94.7667	95.5333	89.1667	0.0962	0.0951	0.1496	0.1420
	0.10	93.8500	95.9667	86.5833	0.0967	0.0951	0.1852	0.1412
	0.50	86.6667	83.9000	81.2667	0.1071	0.1055	0.2513	0.2203
	1.00	90.3167	88.8500	91.2167	0.1713	0.1698	0.4577	0.3648

Table 10: Sensitivity to a choice of significance level  $\alpha = 0.001, 0.005, 0.01, 0.05, 0.1, 0.5$ . The maximum and minimum binsize of PAVA-BC were set to 1200 and 300. The number of bins of quantile-binning and equispaced-binning was set 10.

Test Prevalence	Significant Level	TCE(P)	TCE(Q)	TCE(V)	ECE	ACE	MCE	MCE(Q)
50% (Calibrated)	0.001	1.4500	4.6833	0.1833	0.0138	0.0150	0.1020	0.0528
	0.005	2.4667	5.5667	1.1333	0.0138	0.0150	0.1020	0.0528
	0.010	3.0500	6.2000	1.6500	0.0138	0.0150	0.1020	0.0528
	0.050	7.2833	10.8833	3.4500	0.0138	0.0150	0.1020	0.0528
	0.100	12.8500	15.2000	6.8667	0.0138	0.0150	0.1020	0.0528
	0.500	53.1000	55.3333	46.5667	0.0138	0.0150	0.1020	0.0528
40% (Miscalibrated)	0.001	77.8000	83.3833	76.1000	0.0963	0.0951	0.1466	0.1314
	0.005	86.3000	92.8000	80.0833	0.0963	0.0951	0.1466	0.1314
	0.010	90.1833	95.2167	83.1167	0.0963	0.0951	0.1466	0.1314
	0.050	96.1000	96.4667	88.0667	0.0963	0.0951	0.1466	0.1314
	0.100	97.2167	96.9167	90.1667	0.0963	0.0951	0.1466	0.1314
	0.500	99.3000	98.7167	97.7500	0.0963	0.0951	0.1466	0.1314

Table 11: Comparison of TCE based on the Binomial test and the t-test. TCE(Q)-B denotes TCE(Q) based on the Binomial test and TCE(Q)-T denotes TCE(Q) based on the t-test; the same applies for the other columns. The maximum and minimum binsize of PAVA-BC and the number of bins of quantile-binning and equispaced-binning were varied as in Table 8.

Test Prevalence	Binsize Range	TCE(P)-B	TCE(P)-T	TCE(Q)-B	TCE(Q)-T	TCE(V)-B	TCE(V)-T
50% (Calibrated)	[250, 1000]	3.8000	33.6667	4.2000	31.9167	3.4500	34.2167
	[50, 200]	1.8333	36.0000	4.3000	31.4333	3.4500	34.2167
	[25, 100]	0.2833	31.3667	3.5667	40.4333	3.4500	34.2167
	[5, 20]	7.2833	37.8000	10.8833	41.8500	3.4500	34.2167
	[3, 10]	13.5667	46.5000	38.7500	68.8167	3.4500	34.2167
40% (Miscalibrated)	[250, 1000]	7.7333	50.2833	8.7000	45.1833	88.0667	97.7333
	[50, 200]	45.7667	73.2667	32.2833	71.1667	88.0667	97.7333
	[25, 100]	66.1833	96.5333	56.7667	85.3833	88.0667	97.7333
	[5, 20]	96.1000	99.2667	96.4667	98.4833	88.0667	97.7333
	[3, 10]	96.6000	98.6333	96.7833	98.4833	88.0667	97.7333

Table 12: Comparison of TCE by different total sizes  $N_{\text{test}} = 30, 60, 300, 600, 3000, 6000, 30000, 60000$  of test dataset. The training prevalence was  $P_{\text{training}}(y) = 0.5$  for all datasets. The maximum and minimum binsize of PAVA-BC were set by  $N_{\text{max}} = N_{\text{test}}/20$  and  $N_{\text{min}} = N_{\text{test}}/5$ . The number of bins of quantile-binning and equispaced-binning was set 10.

Test Prevalence	Data Size	TCE(P)	TCE(Q)	TCE(V)	ECE	ACE	MCE	MCE(Q)
50% (Calibrated)	30	0.0000	0.0000	0.0000	0.2293	0.2631	0.4164	0.5660
	60	0.0000	3.3333	0.0000	0.0923	0.2158	0.7148	0.4208
	300	5.3333	11.0000	6.3333	0.0774	0.0867	0.1971	0.2057
	600	1.0000	4.5000	1.6667	0.0368	0.0445	0.3404	0.1270
	3000	8.0667	4.6333	4.7667	0.0190	0.0182	0.1209	0.0304
	6000	7.2833	10.8833	3.4500	0.0138	0.0150	0.1020	0.0528
	30000	16.1633	31.7167	0.7833	0.0036	0.0061	0.9045	0.0164
	60000	19.1483	45.7600	4.4417	0.0035	0.0043	0.0949	0.0100
40% (Miscalibrated)	30	13.3333	6.6667	36.6667	0.3164	0.3377	0.6569	0.6338
	60	0.0000	3.3333	0.0000	0.1072	0.1611	0.7148	0.4208
	300	27.3333	37.3333	48.3333	0.1240	0.1368	0.1971	0.2665
	600	14.1667	8.0000	26.5000	0.0694	0.0685	0.5824	0.1350
	3000	92.2333	91.7667	76.7667	0.0964	0.0958	0.1495	0.1358
	6000	96.1000	96.4667	88.0667	0.0963	0.0951	0.1466	0.1314
	30000	99.4700	99.2300	97.4433	0.0907	0.0906	0.9045	0.1064
	60000	99.7783	99.6600	98.9000	0.0923	0.0923	0.0972	0.1065

Table 13: Comparison of TCE by different prevalences  $P$  of training and test dataset. The training data size was 14000 and the test data size was 6000. The maximum and minimum binsize of PAVA-BC were set to 1200 and 300. The number of bins of quantile-binning and equispaced-binning was set 10.

Train - Test Prevalence	TCE(P)	TCE(Q)	TCE(V)	ECE	ACE	MCE	MCE(Q)	
Calibrated	50% - 50%	7.2833	10.8833	3.4500	0.0138	0.0150	0.1020	0.0528
	40% - 40%	7.5500	16.2167	8.5667	0.0137	0.0191	0.1632	0.0365
	30% - 30%	8.1667	12.8833	2.8167	0.0125	0.0134	0.1042	0.0313
	20% - 20%	15.9500	22.2167	15.9167	0.0173	0.0153	0.6238	0.0370
	10% - 10%	11.9833	16.7833	15.2333	0.0096	0.0114	0.4361	0.0218
	8% - 8%	15.7000	18.5167	23.1500	0.0087	0.0107	0.0700	0.0234
	6% - 6%	11.5333	17.5500	13.9833	0.0035	0.0109	0.3064	0.0195
	4% - 4%	18.5000	15.6667	20.5833	0.0046	0.0074	0.2240	0.0177
2% - 2%	13.1167	11.5500	20.7667	0.0052	0.0059	0.0052	0.0131	
Miscalibrated	50% - 40%	96.1000	96.4667	88.0667	0.0963	0.0951	0.1466	0.1314
	40% - 30%	96.5667	96.1833	82.7500	0.0872	0.0869	0.1485	0.1262
	30% - 20%	94.9500	94.6667	88.5833	0.0846	0.0846	0.2146	0.1247
	20% - 10%	95.8833	95.5833	96.4333	0.0868	0.0868	0.6238	0.1500
	10% - 8%	32.3500	26.7000	42.5667	0.0151	0.0173	0.4361	0.0502
	8% - 6%	42.3167	38.7833	45.8333	0.0164	0.0186	0.3259	0.0477
	6% - 4%	47.0833	39.9500	65.9500	0.0167	0.0188	0.3064	0.0440
	4% - 2%	56.5833	42.4333	72.4500	0.0142	0.0142	0.2240	0.0337
2% - 0%	99.9167	96.9000	100.0000	0.0181	0.0181	0.0181	0.0382	

## C.2 RESULTS ON OTHER UCI DATASETS

Algorithms in Section 4.2 are all trained with the default hyperparameters in the scikit-learn package, except that the maximum depth in the random forest is set to 10 and the number of hidden layers in the multiple perceptron is set to 1 with 1000 units. For better comparison, we add TCE based on quantile bins, denoted TCE(Q) in each table, to five metrics presented in the main text. The following Table 14 compares six different calibration error metrics computed for eight UCI datasets that were not presented in the main text: coil\_2000, isolet, letter\_img, mammography, optimal\_digits, pen\_digits, satimage, spambase [Dua and Graff, 2017, van der Putten and van Someren, 2000-2009, Elter et al., 2007]. The prevalence of the spambase dataset is well-balanced and that of the rest is imbalanced. The following Figures 5 and 6 shows the visual representations of TCE, ECE, and ACE—the test-based reliability diagram and the standard reliability diagram—each for the logistic regression and the gradient boosting algorithm. We selected four datasets, abalone, coil\_2000, isolet, and webpage, to produce the visual representations in Figures 5 and 6.

## C.3 RELIABILITY DIAGRAMS OF RESULTS ON IMAGENET1000

The following Figure 7 shows the visual representations of TCE, ECE, and ACE—the test-based reliability diagram and the standard reliability diagram—for four different deep learning models presented in the main text, where we omit the model ResNet50 whose result sufficiently resembles that of ResNet18.

Table 14: Comparison of six calibration error metrics for five algorithms trained on eight UCI datasets. The same setting of TCE presented in Section 4 is used. TCE(Q) and MCE(Q) denotes TCE and MCE each based on quantile bins where the number of bins is set to 10.

Data	Algorithm	TCE	TCE(Q)	ECE	ACE	MCE	MCE(Q)
coil_2000	LR	8.6189	11.7408	0.0047	0.0111	0.8558	0.0326
	SVM	17.0003	28.9447	0.0071	0.0216	0.4860	0.0381
	RF	22.2260	6.1758	0.0027	0.0125	0.2465	0.0439
	GB	20.8687	12.6569	0.0052	0.0098	0.3738	0.0259
	MLP	98.7445	98.7784	0.0652	0.0578	0.7900	0.1649
isolet	LR	28.8462	27.3932	0.0131	0.0051	0.2183	0.0286
	SVM	11.5812	13.2479	0.0064	0.0028	0.1969	0.0194
	RF	66.4530	52.5214	0.0524	0.0507	0.3635	0.2137
	GB	25.2991	16.6667	0.0198	0.0174	0.4463	0.1123
	MLP	9.8291	17.5641	0.0049	0.0031	0.4173	0.0232
letter_img	LR	10.5167	12.0500	0.0025	0.0008	0.1617	0.0042
	SVM	11.8667	14.8167	0.0019	0.0017	0.6257	0.0146
	RF	26.5000	20.2500	0.0097	0.0033	0.5179	0.0131
	GB	25.9500	18.7333	0.0067	0.0029	0.3653	0.0109
	MLP	19.9833	9.9833	0.0010	0.0001	0.4550	0.0007
mammography	LR	25.0671	26.7660	0.0027	0.0065	0.3594	0.0208
	SVM	20.2683	20.1490	0.0067	0.0088	0.6741	0.0353
	RF	19.4039	9.2996	0.0047	0.0016	0.4465	0.0043
	GB	14.5156	15.4098	0.0061	0.0034	0.5355	0.0124
	MLP	20.5663	26.9747	0.0042	0.0027	0.4351	0.0113
optical_digits	LR	11.6251	27.1649	0.0098	0.0037	0.2251	0.0135
	SVM	4.8043	10.6762	0.0042	0.0028	0.6608	0.0157
	RF	49.6441	38.3155	0.0451	0.0433	0.5432	0.2271
	GB	13.0486	11.2693	0.0181	0.0168	0.5639	0.1122
	MLP	4.6856	12.1590	0.0037	0.0034	0.5992	0.0306
pen_digits	LR	20.4063	23.1049	0.0121	0.0060	0.1652	0.0252
	SVM	9.7635	10.2790	0.0017	0.0010	0.4735	0.0068
	RF	29.6240	22.8623	0.0152	0.0132	0.4535	0.0592
	GB	9.9151	13.0988	0.0077	0.0058	0.6543	0.0303
	MLP	9.4603	10.0061	0.0014	0.0004	0.6457	0.0037
satimage	LR	23.6665	23.0968	0.0215	0.0223	0.7312	0.0767
	SVM	10.2020	21.8540	0.0229	0.0163	0.1666	0.0870
	RF	29.1041	20.1450	0.0265	0.0214	0.2084	0.1328
	GB	23.2004	19.8861	0.0154	0.0235	0.2101	0.0902
	MLP	58.0528	58.4671	0.0352	0.0328	0.5049	0.1384
spambase	LR	33.6713	56.1188	0.0256	0.0267	0.1539	0.0895
	SVM	12.8168	34.5402	0.0177	0.0227	0.2207	0.0465
	RF	66.0391	49.4569	0.0635	0.0601	0.2056	0.1616
	GB	20.2028	20.4200	0.0295	0.0277	0.1409	0.0891
	MLP	60.9703	67.1253	0.0413	0.0397	0.2931	0.1076

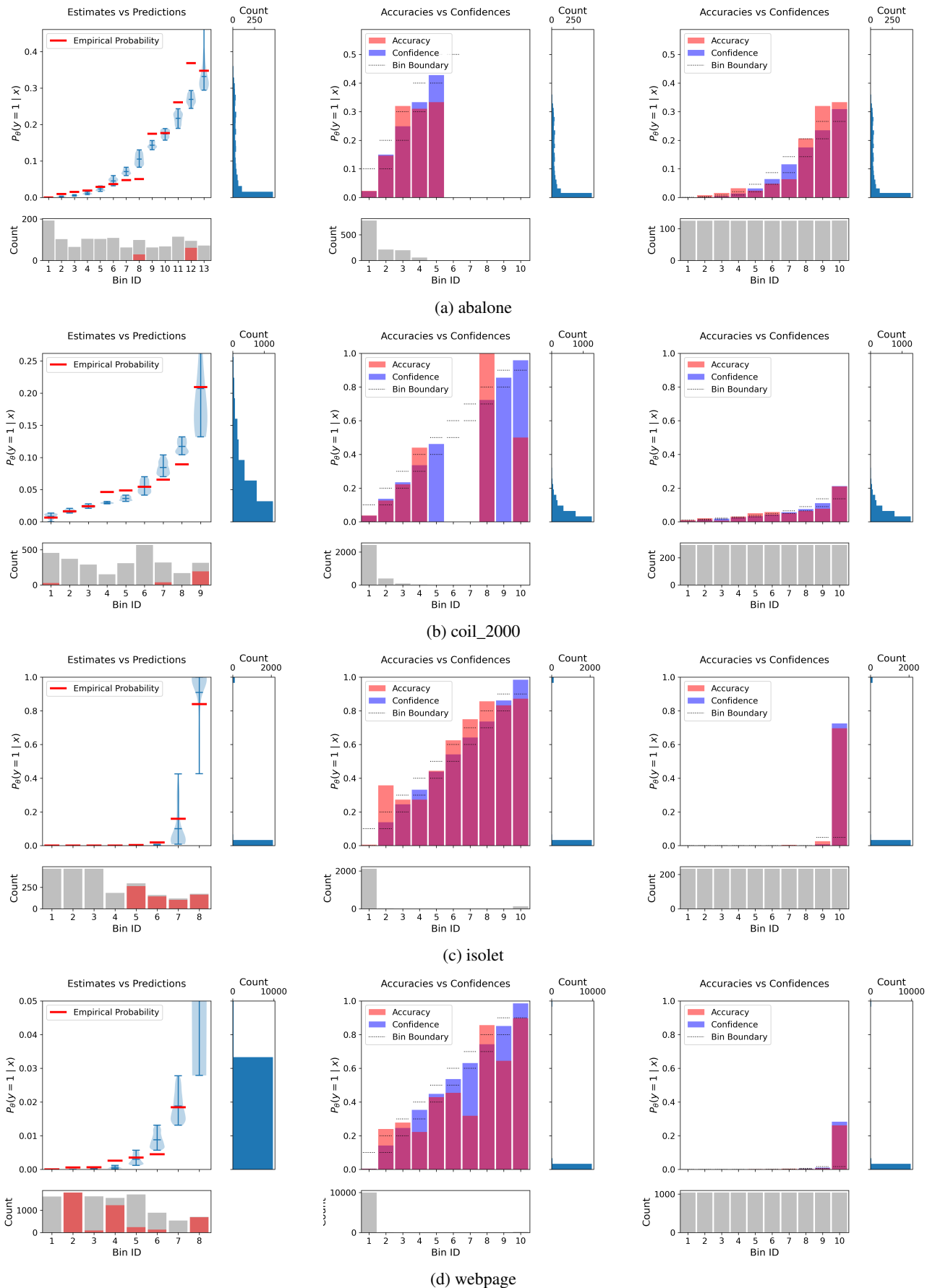


Figure 5: Comparison of visual representations of TCE, ECE and ACE for the logistic regression algorithm. (Left) The test-based reliability diagram of TCE. (Middle) The reliability diagram of ECE. (Right) The reliability diagram of ACE. Each row corresponds to a result on the dataset: (a) abalone, (b) coil\_2000, (c) isolet, and (d) webpage.



Figure 6: Comparison of visual representations of TCE, ECE and ACE for the logistic regression algorithm. (Left) The test-based reliability diagram of TCE. (Middle) The reliability diagram of ECE. (Right) The reliability diagram of ACE. Each row corresponds to a result on the dataset: (a) abalone, (b) coil\_2000, (c) isolet, and (d) webpage.

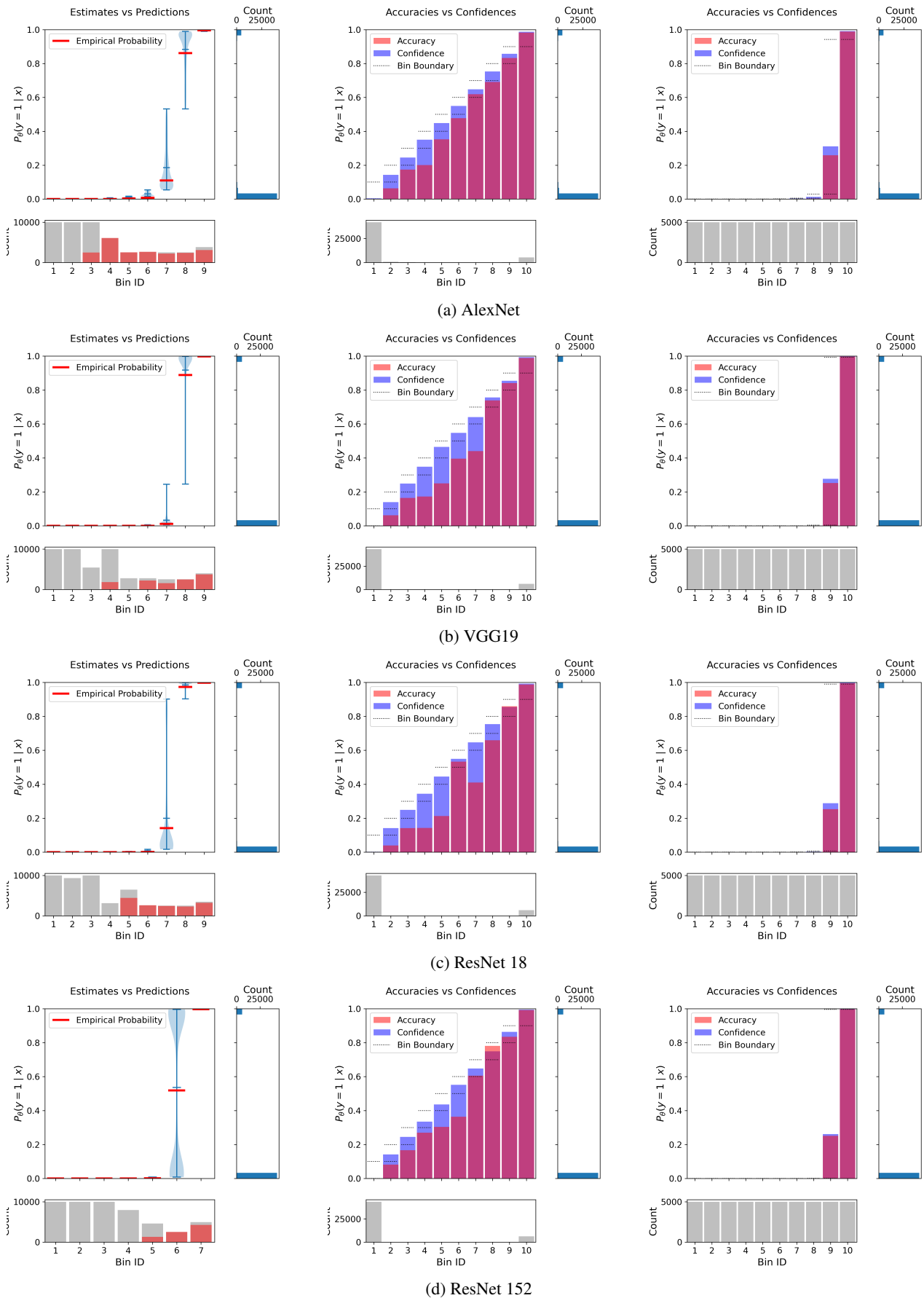


Figure 7: Comparison of visual representations of TCE, ECE, and ACE on the ImageNet 1000 dataset. (Left) The test-based reliability diagram of TCE, (Middle) The reliability diagram of ECE (Right) The reliability diagram of ACE. Each row corresponds to a result for the model: (a) AlexNet, (b) VGG19, (c) ResNet 18, and (d) ResNet 152.